Contact Issues of GaN Technology

D. Qiao, L.S.Yu and S. S. Lau
Department of Electrical and Computer Engineering
University of California, San Diego
San Diego, CA 92093
lau@ece.ucsd.edu

G. J. Sullivan
Rockwell Science Center
Thousand Oaks, CA 91360

S. Ruvimov and Z. Liliental-Weber
Lawrence Berkeley National Laboratory
Berkeley, CA 94720

ABSTRACT

In this paper, we discuss the issue of fabricating reliable and reproducible ohmic contacts on AlGaN HFET structures. During the course of our investigation of fabricating contacts to HFETs, we found that the contact properties could vary significantly from one sample to another, even though they were nominally the same. This problem was prominently manifested in the ohmic contact behavior. The origin of this problem was traced back to the variation of the HFET structure during growth. In this paper, we report an attempt to fabricate reproducible ohmic contacts of these structures.

I. INTRODUCTION

Contact behavior is an important issue in device design and performance. In our laboratory, we have made an attempt to study the contact properties on GaN, AlGaN and AlGaN/GaN HFET structures in a systematic manner. We found that the Schottky barrier heights, ϕ_B^n, between n-GaN and n-$Al_{0.15}Ga_{0.85}N$ differ by about 0.3 eV. For example, the barrier height of Ni on GaN is ~0.95 eV and that on $Al_{0.15}Ga_{0.85}N$ is ~1.27 eV[1]. These are the average values (I-V and C-V) obtained on bulk samples, i.e., the layer thickness of GaN and AlGaN exceeds 1 µm. The barrier height of Ni on HFET structure i.e., $Al_{0.15}Ga_{0.85}N$ (300 Å)/3µm GaN (undoped), cannot be ascertained using the conventional I-V and C-V methods due

https://doi.org/10.1557/S1092578300002234 Published online by Cambridge University Press

to the presence of the piezoelectric donor charge at the AlGaN/GaN interface[2]. Internal photo emission is an alternative way to determine the Schottky barrier height of a metal/AlGaN/GaN heterostructure. In our laboratory, we have measured the barrier height of Ni of $Al_{0.15}Ga_{0.85}N$ (300 Å and 500 Å)/GaN using the internal photo emission technique and obtained a barrier height of ~1.30 eV, independent of the AlGaN layer thickness[3]. This value, well within the experimental scattering range, is considered to be consistent with the value obtained on bulk $Al_{0.15}Ga_{0.85}N$ samples. As the mole fraction of Al in the AlGaN top layer changes to 30%, the barrier height is seen to increase further to ~1.56 eV (see Table 1). These results suggest that the Schottky barrier of HFET structures is largely determined by the upper most AlGaN layer and that the barrier height appears to increase between 0.25 to 0.3 eV for every 15% increment in Al mole fraction in the AlGaN layer up to 30 % of Al. More work is needed to correlate the barrier height and the Al mole fraction in detail.

Table 1. Summary of Schottky barrier height[(a)]

Metal	Material	Ideality n factor	$q\phi_b$ (I-V) (eV)[(e)]	$q\phi_b$ (I-V) (eV)[(f)]	$q\phi_b$ (C-V) (eV)	$q\phi_b$ (photo) (eV)
Ni	Bulk AlGaN[(b)]	1.23	1.03	1.25	1.26	1.28
Ni	GaN	1.14	0.84	0.95	0.96	0.91
Ni	HFET[(c)]					1.31
Ni	HFET[(d)]					1.56
Ti	Bulk AlGaN[(b)]	1.08	0.79	0.84	1.10	
Ti	GaN	1.08	0.60	0.65	0.68	

[(a)]The data (I-V and C-V) are the average value from 15 diodes; the standard deviation is about 0.05 for both of the *n* factor and the barrier heights.

[(b)]Al mole fraction was 15% in the AlGaN samples.

[(c)]$Al_{0.15}Ga_{0.85}N$ (300 Å or 500 Å)/3µm undoped GaN.

[(d)] $Al_{0.3}Ga_{0.7}N$ (500 Å)/3µm undoped GaN.

[(e)] Calculated from Equation 1;

$$I = AA^{*}T^{2}e^{-q\phi_{b}/kT}\left(e^{qV/nkT}-1\right) \tag{1}$$

[(f)] Calculated from Equation 1 and corrected by equation 2;

$$\phi_{bc} = n\phi_{b} - (n-1)\frac{kT}{q}\ln\frac{N_{c}}{N_{d}} \tag{2}$$

https://doi.org/10.1557/S1092578300002234 Published online by Cambridge University Press

We have also been investigating the ohmic behavior on the III-V nitrides. Of particular interest to us was understanding how to fabricate low resistance and reproducible ohmic contacts on HFET structures. During the course of the study, we found that the ohmic behavior varied significantly from one wafer to another, even though these wafers were nominally the same, i.e., n- $Al_{0.15}Ga_{0.85}N$ (300 Å)/ $Al_{0.15}Ga_{0.85}N$ (30 Å, undoped)/i-GaN(1 μm). Table 2 shows the results of the measured contact resistivity on four different wafers with nominally the same structure. The $n_s\mu$ product, extracted from Hall effect measurements, is the usual parameter that characterizes the HFET samples (see Table 2). For samples with a large value of $n_s\mu$ product, the contact resistance should be low, compared to samples with a small $n_s\mu$ value, at least in principle. This is because the $n_s\mu$ product is believed to indicate good electrical conduction in the channel region and should lead to low ohmic contact resistance. According to this idea, sample #4, in Table 2 should yield the lowest contact resistance, since it had the largest value of $n_s\mu$; and sample 2 with the smallest $n_s\mu$ should yield the largest contact resistance. Contact resistance measurement using the TLM method indicated that sample #4 had the highest contact resistivity (2.07E-3 $\Omega\cdot cm^2$), and sample #2 had a low contact resistivity of 4E-6 $\Omega\cdot cm^2$. This behavior was not expected and could not be explained by the $n_s\mu$ product value alone.

Table 2. Contact resistance and parameters of nominally the same AlGaN/GaN HFET structures ($Al_{0.15}Ga_{0.85}N$(300 Å)/GaN(1 μm)/sapphire)[a]

Samples	$n_s\mu$ E16 $(V\text{-}s)^{-1}$	R_c[b] $\Omega\cdot mm$	ρ_s[c] $\Omega\cdot cm^2$	R_s[d] Ω/	Al fraction in the AlGaN layer, %		Thickness of the AlGaN layer, Å	
					SIMS[e]	EDX[f]	SIMS	TEM[g]
#1	1.20	0.22	8.60E-7	830	9	11-15.2	220	210
#2	0.74	0.50	4.00E-6	990	10	~25.3	360	280
#3	1.09	3.73	2.05E-4	770	15	22-25.4	360	280
#4	1.34	15.25	2.07E-3	1190	22	30	600	340

[a]The contact metallization was Al(710 Å)/Ti(300 Å)/HFET annealed at 950 °C for 80 seconds in flowing N_2. The thickness of AlGaN and the Al fraction can vary significantly from one sample to another, even though they were nominally the same. These parameters can also vary but to a lesser extent when different analytical methods were used for the same sample.

[b]R_c: Contact resistance.

[c]ρ_s: Specific contact resistivity.

[d]R_s: sheet resistance.

[e]SIMS: Secondary ion mass spectroscopy.

[f]EDX: Energy dispersive x-ray.

[g]TEM: Transmission electron microscopy.

https://doi.org/10.1557/S1092578300002234 Published online by Cambridge University Press

Structural and chemical analysis of the samples showed that these four nominally identical samples were in fact very different in the Al mole fraction and in thickness in the AlGaN layer. Sample #4 had an Al mole fraction of 22% (SIMS value, believed to be more accurate than EDX) in the AlGaN layer with a thickness of 340 Å (TEM value, believed to be more accurate than SIMS). This sample had the largest contact resistivity (2E-3 $\Omega\cdot cm^2$). Sample #1 had an Al mole fraction of 9% in the AlGaN layer with a thickness of 210 Å, and yielded the smallest contact resistivity (8.6E-7 $\Omega\cdot cm^2$). Table 2 suggests that the contact behavior is primarily governed by the Al mole fraction and the thickness of the top AlGaN layer in these nominally identical samples. This observation led us to conclude that the control of the growth of the HFET samples is far from satisfactory. We, further, assume that sample non-uniformity is a common problem in almost all nitride growth systems.

II. APPROACHES TO FABRICATE LOW RESISTANCE-CONTACT IN A MORE CONSISTENT MANNER

We considered two approaches to improve the consistency of low resistance contact behavior in HFET structures where sample non-uniformity is expected. The first approach was to use Si implantation into the HFETs to increase the electron concentration to facilitate carrier tunneling across the contact[4-8]. We picked sample #4 (the worst case) in Table 2 as a test vehicle to examine the implantation approach; we assumed that if the contact behavior on sample #4 could be improved, then all other samples could be improved using the same approach. In using this approach, we divided sample #4 into two groups. For group 1 (samples #4C-1 and #4A-1), Si^{28} was directly implanted into the HFET structure at 40 keV with a dose of 1E16 cm^{-2}. The projected range, R_p, was estimated, using TRIM96, to be about 600 Å into the sample with a peak concentration of about 1.4E21cm^{-3}. After implantation, a layer of AlN, used as a capping layer for dopant activation, with a thickness of about 1800 Å was sputter-deposited onto the samples. For group 2 (samples #4C-2 and #4A-2), a layer of 1800 Å thick AlN was first deposited onto the samples, followed by Si implantation through the AlN layer at 120 keV with a dose of 1E16cm^{-2}. The estimated location of the peak concentration (6.2E20cm^{-3}) was about 340 Å into the HFET sample. The advantage of implanting through the AlN capping layer was the ability to place the R_p closer to the HFET surface region; the disadvantages include the loss of some implanted Si ions when the AlN capping layer is removed and the possibility of ion-mixing some Al into the AlGaN layer, thus changing the HFET top layer composition. Samples #4C-1, 4C-2, 4A-1 and 4A-2 were then annealed at 1150 ^oC for 30 seconds to activate the implanted Si, followed by removing the AlN capping layer using hot phosphoric acid. TLM patterns were then fabricated for contact resistance measurements. A conventional Al (710 Å)/Ti(300 Å)/HFET[9] metallization was e-beam deposited onto the two groups of implanted samples. The samples were coated with AlN (~1000 Å thick) as an encapsulation layer to prevent the oxidation during ohmic annealing.

It has been shown that Ti-based metallization schemes reduce contact resistance by forming a metallic $AlTi_2N$ layer with AlGaN, leaving an N-deficient AlGaN region, believed to be heavily n-type, beneath the $AlTi_2N$ contact layer[9]. Fig. 1(a) shows a cross-sectional electron microscopy image of sample #4C. The contact layer contains two sublayers of different contrast due to different Al/Ti ratio in the sublayers. EDX analysis indicates that the composition of the top sublayer is close to Al_3Ti, in good agreement with previous results, while the interfacial layer (with darker shading) is rich in Ti (with Ti/Al ~ 2). Table 3 shows the contact resistance for the conventional metallization (Al (710 Å)/Ti (300 Å)/HFET) on non-implanted samples

https://doi.org/10.1557/S1092578300002234 Published online by Cambridge University Press

(sample #4C), direct implanted samples (sample #4C-1) and implanted through the AlN (sample #4C-2).

Table 3. Contact Resistance for the conventional metallization (Al(710Å)/Ti(300Å))[a]

		R_c Ω·mm	ρ_s Ω·cm^2	R_s Ω/
#4C	No implantation	15±3	(2.1±0.8)E-3	1200±300
#4C-2	120 keV, 1E16 cm^{-2}, implantation through AlN	4.9±0.2	(1.9±0.6)E-3	140±40
#4C-1	40 keV, 1E16 cm^{-2}, direct implantation	1.1±0.1	(1.4±0.4)E-4	90±15

[a]The implantation activation was done at 1150 ^{o}C for 30 seconds with an AlN capping layer in flowing N_2. The contact formation was done at 950 ^{o}C for 80 seconds.

It is clear that direct implantation and activation at 1150 ^{o}C for 30 seconds significantly reduced the sheet resistance of the HFET from 1200 Ω/ to 90 Ω/ , in spite of the relatively low activation temperature of 1150 ^{o}C. As a result, the contact resistance R_c reduced from ~15 Ω·mm (non-implanted sample) to ~1.1 Ω·mm for directly implanted samples. This is because R_c is related to the sheet resistance by the following relationship:

$$R_c = \sqrt{\rho_s R_s}\ , \tag{3}$$

where R_c (Ω·mm) is the contact resistance, R_s (Ω/) is the sheet resistance of the semiconductor beneath the contact and ρ_s (Ω·cm^2) is the specific contact resistivity at the metal/semiconductor interface. While the values of R_c for the implanted samples seemed to decrease substantially, depending on the implantation scheme, compared to those of non-implanted samples, the specific contact resistivity, ρ_s, did not decrease as impressively. This is primarily due to the inability of carrier tunneling through the remaining un-reacted AlGaN layer, using a relatively thin Ti(300Å) in the metallization scheme. Increasing the annealing time at 950 ^{o}C with and without an AlN capping layer did not improve the contact further beyond 80 seconds of annealing, apparently the reaction has reached an end point after 80 seconds of annealing.

To improve the specific contact resistivity, ρ_s, it is necessary to reduce the thickness of the un-reacted AlGaN layer for easier access to the GaN layer underneath. Based on this concept, we used a different Al(200 Å)/Ti(1500 Å) ratio for the contact formation. In this case, the Ti layer was much thicker and would consume more AlGaN to form $AlTi_2N$, thereby resulting in a much thinner (or none at all) un-reacted AlGaN for easy carrier tunneling. This scheme is referred to as the "advancing metallization" here. In the conventional scheme, 710 Å of Al reacts with 250 Å of Ti to form Al_3Ti at 250 ^{o}C to 300 ^{o}C, leaving an excess Ti layer 50 Å thick to react with the AlGaN layer. For samples with thicker AlGaN layers (≥300 Å) and with a high Al fraction (≥20%), the conventional Al(710 Å)/Ti(300 Å) metallization does not yield satisfactory contact resistance. There may be two possible reasons for this: (1) the chemical reactivity decreases with increasing Al fraction in the AlGaN layer, since AlN appears to be more stable at high temperatures than GaN; (2) for thick AlGaN with a high Al fraction, 50 Å of excess Ti is

https://doi.org/10.1557/S1092578300002234 Published online by Cambridge University Press

not enough to consume most of the AlGaN top layer, leaving a relatively thick un-reacted AlGaN layer at the interface to hinder carrier tunneling due to its high Schottky barrier height and thickness.

Using the “advancing” scheme, Al and Ti react to form Ti_3Al (not Al_3Ti as in the conventional scheme) at 200-400 ^oC, leaving 850 Å of Ti in excess to fully react with the AlGaN layer to form the $AlTi_2N$ phase. This reaction would leave little or no AlGaN layer left in the HFET source and drain region, thus resulting in efficient carrier tunneling and much reduced specific contact resistivity, ρ_s.

Since the upper most contact layer is probably Ti_3Al (not Al_3Ti), a capping layer of AlN is required for the ohmic annealing at 950 ^oC for 10 minutes to prevent oxidation (5 minutes was found to be insufficient to react fully). Pure Ti capped with an AlN layer was not practical due to the ease of oxidation of un-reacted Ti after the removal of AlN even at room temperature in air. For the conventional Al(710 Å)/Ti(300 Å) scheme, the top Al_3Ti layers has been found to be stable when annealed at 950 ^oC for 80 seconds in N_2 with little oxidation.

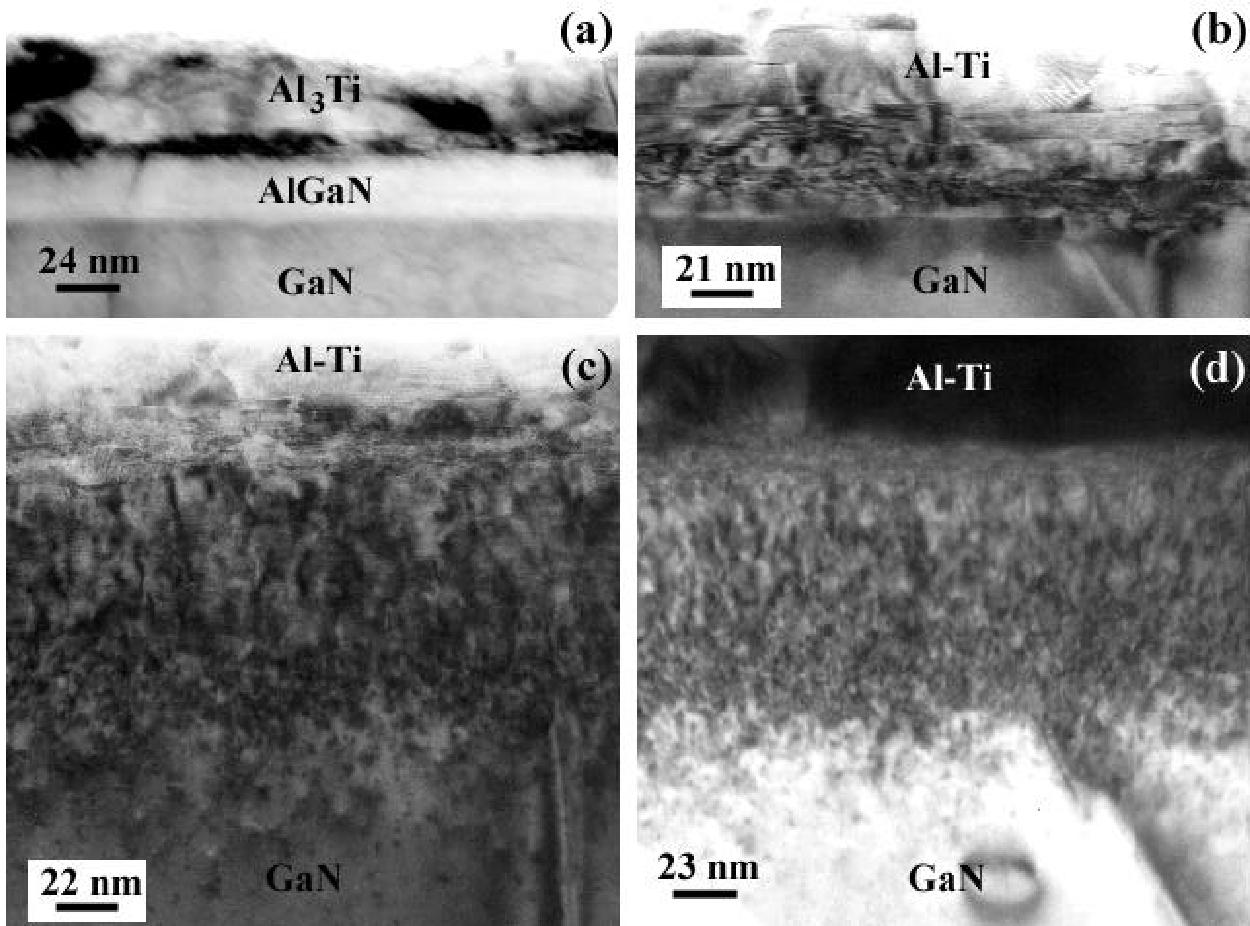

Fig. 1. TEM cross sectional view of samples (a) 4C, (b) 4A, (C) 4A-1 and (d) 4A-2.

https://doi.org/10.1557/S1092578300002234 Published online by Cambridge University Press

Fig. 1 (b) shows the cross-sectional TEM image of the sample with the "advancing" Al(200 Å)/Ti(1500 Å) contact (#4A). It is clear that the AlGaN layer is partially and sometimes completely consumed due to the reaction with Ti. It also can be found that the reaction is enhanced at the dislocations intersecting the AlGaN layer. Fig. 1(c) shows the cross-sectional TEM image of the sample with the "advancing" contact and the direct Si implantation prior to the metallization (#4A-1). Fig. 1(d) shows the image of the sample with the "advancing" contact and the Si implantation through a layer of AlN prior to the metallization (#4A-2). For these two samples, the contact layer contains two sublayers of different structure and composition, suggesting the reaction of the metal (presumably Ti) with AlGaN. The AlGaN layer is hardly visible on the TEM images of Figures 1(c) and (d) due to a high defect density in the HFET structure caused by the ion implantation. However, it seems that the AlGaN layer is less consumed in the samples #4A-1 (directly implanted) and #4A-2 (implanted through a layer of AlN) compared to sample #4A (not implanted). The damaged region, containing a high density of dislocation loops, is almost polycrystalline in the region close to the metal contact. This polycrystalline region differs in length and in average grain size for the direct and through-AlN implantation. The average grain size is about 50 Å and 110 Å for samples #4A-1 and #4A-2, respectively. TEM results suggest that both the sheet resistance, R_s, and the specific contact resistivity, ρ_s, may be affected by the remaining AlGaN layer and by the ion-implantation damage of crystalline lattice and possible diffusion of Ti through grain boundaries.

Table 4 summarizes the TLM results obtained on the samples with the "advancing" Al(200 Å)/Ti(1500 Å) metallization scheme. For the advancing scheme, the contact resistance and the specific contact resistivity were much smaller compared to those obtained with the conventional metallization scheme. The samples using a combination of direct implantation and the "advancing" metallization gave the lowest contact resistance, R_c, of 0.25 Ω·mm or 5.6×10^{-6} $\Omega\cdot cm^2$.

The drastic decrease in R_c is due to the reduction in sheet resistance R_s caused by the Si implantation and the reduction of ρ_s caused by the "advancing" metallization scheme. Both of these factors contribute to the reduction of R_c.

A comparison of Table 3 and Table 4 shows the advantage of using the "advancing" metallization scheme to reduce contact resistance. However, results shown in Table 2 indicate that the conventional Al(710 Å)/Ti(300 Å) system can form low resistance contacts quite readily on HFET structures with a thin AlGaN top layer and a low Al fraction.

Table 4. Contact Resistance for the "advancing" metallization (Al(200 Å)/Ti(1500 Å)) [(a)]

		R_c Ω·mm	ρ_s $\Omega\cdot cm^2$	R_s Ω/
#4A	No implantation	1.8±0.3	(5±1)E-5	660±50
#4A-2	120 keV, 1E16 cm^{-2}, implantation through AlN	0.37±0.01	(1.0±0.1)E-5	129±3
#4A-1	40 keV, 1E16 cm^{-2}, direct implantation	0.25±0.01	(5.6±0.9)E-6	110±10

[(a)]The implantation activation was done at 1150 °C for 30 seconds with an AlN layer in flowing N_2. The contact formation was done at 950 °C for 10 minutes, with an AlN capping layer.

In summary, Si implantation into HFET structures was found effective in reducing the sheet resistance, R_S, of the structure. With annealing temperatures higher than 1150 °C, the sheet resistance is expected to decrease even more. The "advancing" metallization scheme of Al(200

https://doi.org/10.1557/S1092578300002234 Published online by Cambridge University Press

Å)/Ti(1500 Å) reduced the specific contact resistivity, ρ_s. Combining direct implantation of Si and the "advancing" metallization, very low contact resistance (~0.25 Ω·mm) and low specific contact resistivity, ρ_s, (~5.6×10^{-6} $\Omega\cdot cm^2$) was achieved on HFET structures with an AlGaN layer at least as thick as 340 Å and with an Al fraction at least as large as 22%.

ACKNOWLEDGMENT

This study was supported by BMDO (Dr. K. Wu) monitored by the US Army Space and Strategic Defense Command. UCSD would like to acknowledge the National Science Foundation for support.

REFERENCES

[1]. L.S. Yu, D. J. Qiao, Q. J. Xing, S.S. Lau, K.S. Boutro and J.M. Redwing, Appl. Phys. Lett. **73**, 238 (1998).

[2]. C.H. Chen, S.M. Baier, D.K. Arch and M.S. Shur, IEEE Tran. Electron Device, **35**, 571 (1988).

[3]. E.T. Yu, X.Z. Dang, L.S. Yu, P.M. Asbeck, S.S. Lau, K.S. Boutros and J.M. Redwing, Appl. Phys. Lett. **73**, (1998).

[4]. J.C. Zopler, D.J. Rieger, A.G. Baca, S.J. Pearton, J.W. Lee, R.A. Stall, Appl.Phys. Lett. **69**, 538 (1996).

[5]. X.A. Cao, F. Ren, S.J. Pearton, A. Zeitouny, M. Eizenberg, J.C. Zolper, C.R. Aberbathy, J. Han, R.J. Shul and J.R. Lothian, Appl.Phys. Lett., **73**, 229(1998).

[6]. Jinwook Burm, Kenneth Chu, William A. Davis, William J. Schaff , Lester F. Eastman, Tyler J. Eustis, Appl.Phys. Lett., **70**, 464(1997).

[7]. J.C. Zolper, J. Han, R.M. Biefeld, S.B. Van Deusen, W.R. Wampler, D.J. Reiger, S.J. Pearton, J.S. Williams, H.H. Tan, and R. Stall, J. Electron. Mater., **27**, 179 (1998).

[8]. H. Kobayashi and W.M. Gibson, Appl. Phys. Lett., **73**, 1406, 1998.

[9]. S. Ruvimov, Z. Liliental-Weber, J. Washburn, D. Qiao and S.S. Lau, Appl. Phys. Lett. **73**, 2582 (1998).

https://doi.org/10.1557/S1092578300002234 Published online by Cambridge University Press